Electronic Supplementary Information(ESI)

Title: Heterogeneous tissue construction by on-demand bubble-assisted acoustic patterning

*Qinghao Hu,[ab] Xuejia Hu,[c] Yang Shi,[d] Li Liang,[ab] Jiaomeng Zhu,[ab] Shukun Zhao,[ab] Yifan Wang,[ab] Zezheng Wu,[a] Fubing Wang ,[e] Fuling Zhou,[f] and Yi Yang [*ab]*

a. Department of Clinical Laboratory, Institute of Medicine and Physics, Renmin Hospital, Key Laboratory of Artificial Micro- and Nano- Structures of Ministry of Education, School of Physics & Technology, Wuhan University, Wuhan 430072, People's Republic of China Shenzhen Research Institute, Wuhan University, Shenzhen 518000, China

b. Shenzhen Research Institute, Wuhan University, Shenzhen 518000, People's Republic of China

c. Department of Electronic Engineering, School of Electronic Science and Engineering, Xiamen University, Xiamen 361005, People's Republic of China

d. Institute of Nanophotonics, Jinan University ,Guangzhou 510632, China

e. Department of Laboratory Medcine, Zhongnan Hospital, Wuhan University, Wuhan 430071, China

f. Department of Hematology, Zhongnan Hospital, Wuhan University, Wuhan 430071, China

* Tel.: 86-027-6875 2989 (office)

Email: yangyiys@whu.edu.cn

This PDF file includes:

Figures S1 to S4: Bubble-assisted patterning of liver lobule chips (Figure S1); 3D morphological characterisation of the bubbles captured by the pits(Figure S2); Two different pits arrays capturing bubbles(Figure S3).Characterisation of the properties of hydrogels(Figure S4); the process of making a model of liver lobules(Figures S5); and cell growth in hydrogels(Figures S6); additional fomular note (PDF).

Other supplementary materials for this manuscript include the following:

Movie S1: Motion of the PS ball along the acoustic vortex line (MP4);

Movie S2: The large-area patterned process of the hepatic lobules on a chip (MP4);

Movie S3: Patterned process of the hepatic lobules on a chip(detail) (MP4)

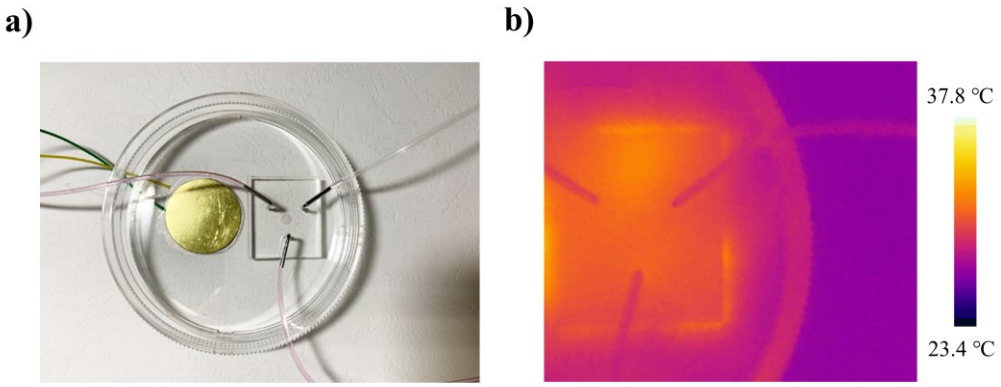

Figure S1. Bubble-assisted acoustic cell patterning chip. a) Bubble-assisted acoustic patterning microfluidic chip fixed on a Petri dish; b）Infrared thermography of a chip undergoing cell patterning process

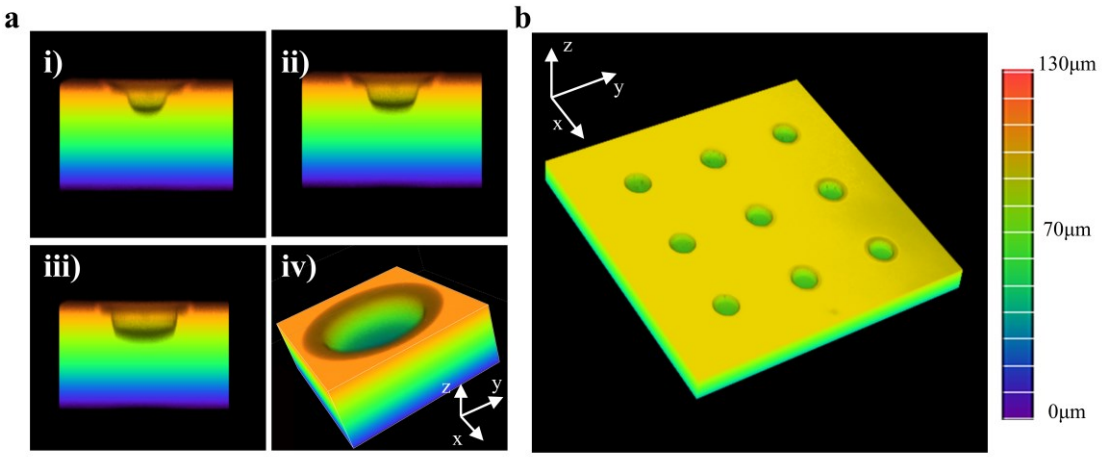

Fig S2. 3D Morphological characterisation of the bubbles captured by the pits. a) iv) shows a 3D detail of a single bubble shape; where Fig a)i), ii) and iii) show sections at different locations respectively. Figure b) shows a 3D scan of the captured bubble array

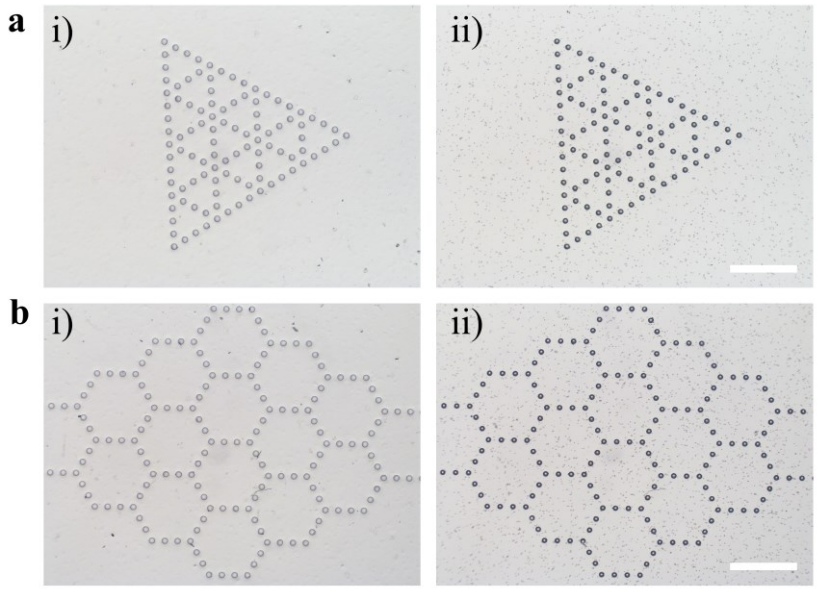

Fig S3. Two different pits arrays capturing bubbles. a)i) and b)i): diagrams of the chip structure without cell suspension injection; Scale bar:500μm b)ii) and a)ii): diagrams of the bubble array formed by pits capturing bubbles after cell suspension injection，Scale bar:500μm.

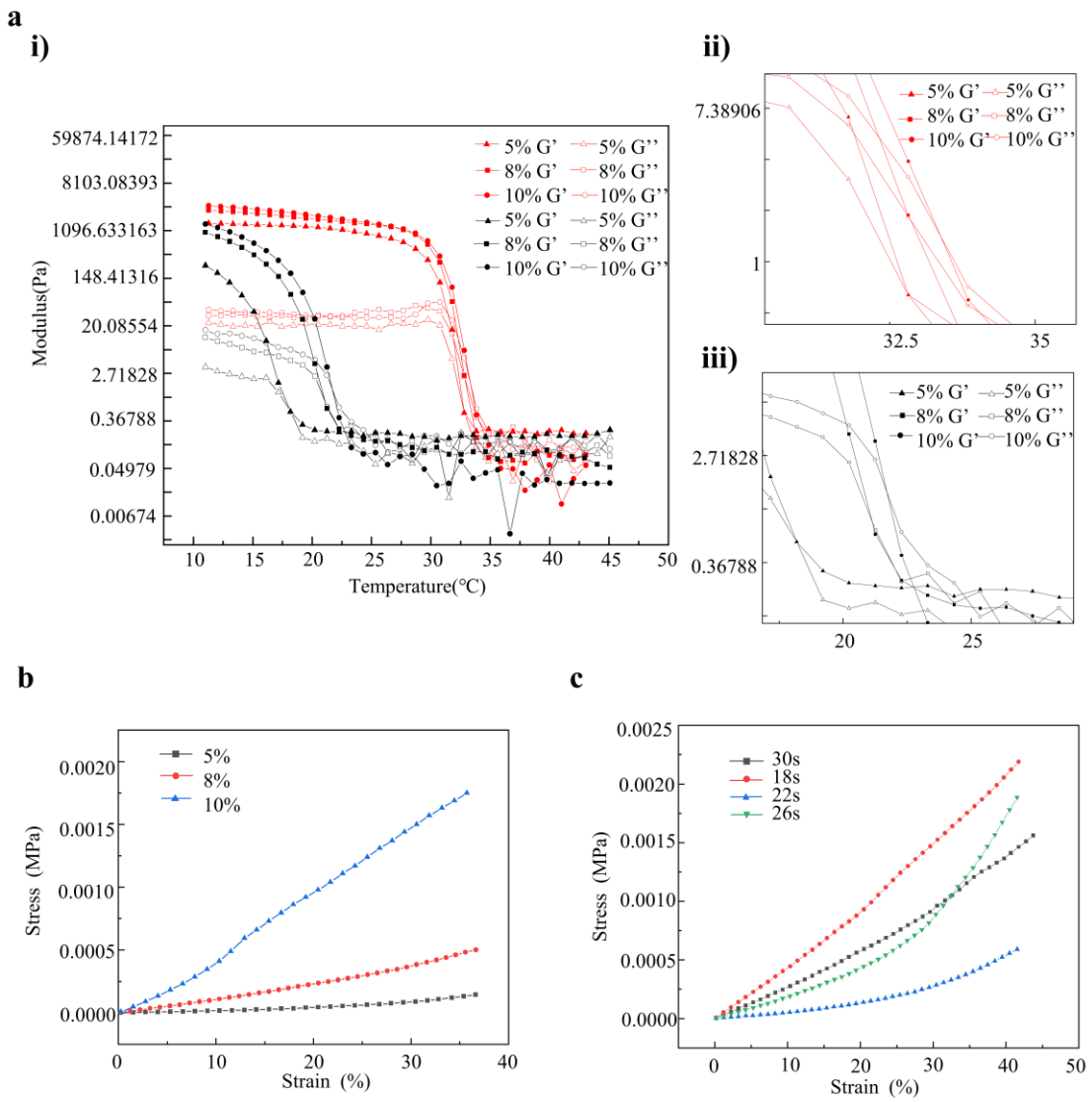

Figure S4 Characterisation of hydrogel properties. a) i) Phase change scanning process for cooling and warming of Gelma60 hydrogels with concentrations of 5%, 8% and 10% respectively. Rising/lowering scan range: 4°C-40°C; temperature scan rate: 2°C/min; black represents the cooling process, red represents the warming process. The temperature at the intersection of the energy storage modulus and the loss modulus during the phase change process is the phase change temperature. ii) Enlarged view of the local area of the warming phase change point (solid to liquid); iii) Enlarged view of the local area of the cooling phase change point (liquid to solid);b) Compression modulus curves for 30s curing of hydrogels of different concentrations; c) Compressive modulus curves for gelma hydrogels with 8% concentration at different times of light curing

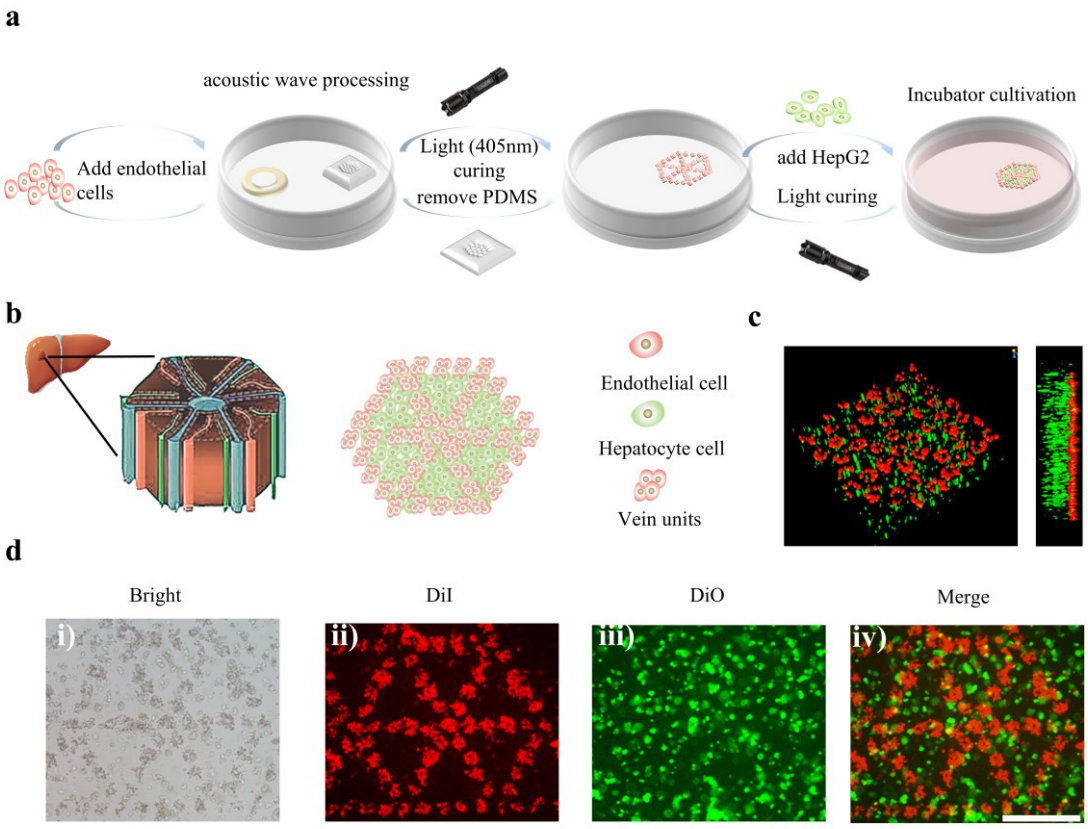

Figure S5 Fabrication of in vitro models of hepatic lobules. a) Schematic diagram of experimental production process of hepatic lobule model in vitro; b) Animation model of actual hepatic lobule structure (left); Image of liver lobule model in vitro (right); c) Three-dimensional fluorescence of an in vitro model of hepatic lobule obtained by confocal scanning; d) Structural characterization of the hepatic model. Scale bar : 500 μm i) Bright field image of liver lobule model in vitro; ii) The fluorescence diagram of hepatic lobule model excited by green light shows the endothelial cells labeled by orange fluorescent probe; iii） The fluorescence diagram of hepatic lobule model excited by blue light shows the liver cancer cells labeled by green fluorescent probe; iv) Figure iv) merged from Figure ii) and figure iii) by ImageJ.

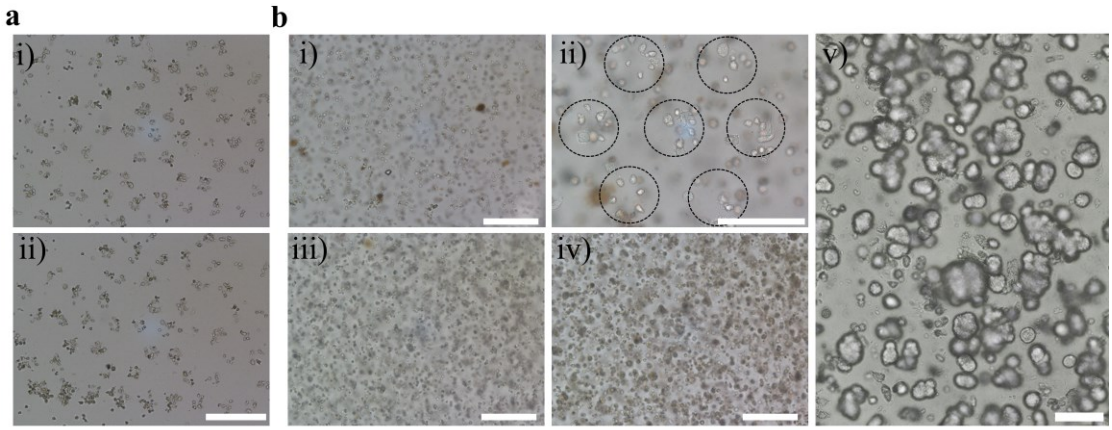

Figure S6 Growth of cells in hydrogels. a) Individual culture of patterned endothelial cells; Scale bar:200 μm i)0day ii)1day; b) Culture of liver lobule models i) 0day ,Scale bar:200 μm ; ii) A partial magnification after 1 day of culture, you can see that the endothelial cells have started to extend their tentacles (marked by black circles) , Scale bar:100 μm ; iii) By the third day of culture, the liver cancer cells showed significant proliferation, Scale bar:200 μm ; iv) Accelerated proliferation of hepatocellular carcinoma cells by day 5 of culture. Scale bar:200 μm ; v) A partial magnification of the culture up to day 7 shows that the hepatocellular carcinoma cells are proliferating and proliferating in clusters. Scale bar:100 μm.

Additional equations notes

(The equations in the text are also listed here to help the reader understand them in a logical order)

$$\boldsymbol{F_{Drag} = 6\pi\mu r_p v_p} \quad (1)$$

Where μ represents the dynamic viscosity, r denotes the radius of cells, v implies the relative velocity of particles, and the subscript p signifies the cells or particle.

$$\boldsymbol{F_{Drag}(max) = 6\pi\mu r_p v_m} \quad (2)$$

$$\boldsymbol{v_m = \omega^{-1}\varepsilon^2 r^4 d^{-5}} \quad (3)$$

Where ω implies the angular frequency; ε denotes the bubble displacement; r is radius of the bubble and d represents the centre-to-centre interval between the bubble and the cells (particle).

$$\boldsymbol{F_R = \frac{4}{3}\pi\rho_M B \cdot \frac{r^4 {r_p}^3}{d^5}\omega^2\varepsilon^2} \quad (3)$$

$$\boldsymbol{B = 3 \cdot \frac{(\rho_S - \rho_M)}{2\rho_S + \rho_M}} \quad (4)$$

where ρ_s is the cell density, ρ_M is the medium density and B determines the direction of the acoustic radiation force ($\rho_s > \rho_M$, $B > 0$, particles are attracted into the bubble; $\rho_s < \rho_M$, $B < 0$, particles are repelled away from the bubble).

$$\boldsymbol{\frac{F_{Drag}(max)}{F_R} = \frac{9}{4}\frac{\mu}{\pi B \rho_M} f^{-1} r_p^2} \quad (5)$$

For a given device, μ, B and ρ_M in equation (5) are constants. z_s is defined by the cells in the selection set. Optimising f is therefore crucial for the performance of the device.

$$\boldsymbol{f_n^2 \approx \frac{1}{4\pi^2}(n-1)(n+1)(n+2)\frac{\sigma}{\rho_M r}} \quad (6)$$

where f_n is the resonant frequency in oscillation mode n and σ is the surface tension of the medium.